Atmos. Meas. Tech. Discuss., 2, 1663–1692, 2009
www.atmos-meas-tech-discuss.net/2/1663/2009/
© Author(s) 2009. This work is distributed under
the Creative Commons Attribution 3.0 License.

Atmospheric Measurement Techniques Discussions

Atmospheric Measurement Techniques Discussions is the access reviewed discussion forum of *Atmospheric Measurement Techniques*

Determination of an effective trace gas mixing height by differential optical absorption spectroscopy (DOAS)

B. Zhou[1], S. N. Yang[1], S. S. Wang[1], and T. Wagner[2]

[1]Department of Environmental Science and Engineering, Fudan University, Shanghai, China
[2]Max Planck Institute for Chemistry, Mainz, Germany

Received: 2 July 2009 – Accepted: 7 July 2009 – Published: 20 July 2009

Correspondence to: B. Zhou (binzhou@fudan.edu.cn)

Published by Copernicus Publications on behalf of the European Geosciences Union.

Abstract

A new method for the determination of the Mixing layer Height (MH) by the DOAS technique is proposed in this article. The MH can be retrieved by a combination of active DOAS and passive DOAS observations of atmospheric trace gases; here we focus on observations of NO_2. Because our observations are sensitive to the vertical distribution of trace gases, we refer to the retrieved layer height as an "effective trace gas mixing height" (ETMH). By analyzing trace gas observations in Shanghai over one year (1017 hourly means in 93 days in 2007), the retrieved ETMH was found to range between 0.1 km and 2.8 km (average is 0.78 km); more than 90% of the measurements yield an ETMH between 0.2 km and 2.0 km. The seasonal and diurnal variation of the ETMH shows good agreement with mixing layer heights derived from meteorological observations. We investigated the relationship of the derived ETMH to temperature and wind speed and found correlation coefficients of 0.65 and 0.37, respectively. Also the wind direction has an impact on the measurement to some extent. Especially in cases when the air flow comes from highly polluted areas and the atmospheric lifetime of NO_2 is long (e.g. in winter), the NO_2 concentration at high altitudes over the measurement site can be enhanced, which leads to an overestimation of the ETMH. Enhanced NO_2 concentrations in the free atmosphere and heterogeneity within the mixing layer can cause additional uncertainties. Our method could be easily extended to other species like e.g. SO_2, HCHO or Glyoxal. Simultaneous studies of these molecules could yield valuable information on their respective atmospheric lifetimes.

1 Introduction

Pollutants emitted into the atmospheric boundary layer are dispersed horizontally and vertically through atmospheric turbulence and convection, and finally can become completely mixed over this layer that is widely known as "mixing layer". Mixing height (MH) has a close relation to meteorological conditions, and meanwhile is a key input pa-

AMTD
2, 1663–1692, 2009

rameter to many air quality forecast models. MH determines the volume available for the dispersion of pollutants, so it is of particular importance in the prediction models of pollutants concentration. However, the MH is not a meteorological parameter that can be directly measured, and moreover the determination and assessment of it is still difficult.

There are two main approaches available for the estimation of MH. One is through analyzing profiles of meteorological parameters, such as temperature, pressure, humidity, and aerosol, and the profiles are attained with remote sensing techniques such as Radiosoundings, tethered balloon, mast, doppler weather radar/wind profiler, Lidar, and Sodar. MH could also be retrieved by analyzing temperature and pressure profiles from temperature and pressure sensors on commercial planes. Each method has its own advantages and disadvantages, because they can not give attention to all the aspects such as observing range, temporal and spatial resolution, measurement precision, instrument and operation cost (Seibert et al., 2000).

The second approach makes use of models based on meteorological data. The first method can provide high temporal and spatial resolution information on the MH. Although widely used, the latter may entail uncertainties in the estimation of MH as discussed by certain authors (He et al., 2006; Berman et al., 1997; García, 2007).

In this study we introduce a new technique for the estimation of the MH, which is directly related to the mixing processes of pollutants. The method is based on a combination of active and passive differential optical absorption spectroscopy (DOAS) observations of NO_2 (also other trace gases could be used). Because our observations are sensitive to the vertical distribution of trace gases, we refer to the retrieved layer height as an "effective trace gas mixing height" (ETMH).

Since introduced in the 1970s (Perner and Platt, 1979; Noxon, 1975; Platt, 1994; Evangelisti et al., 1995; Solomon et al., 1999), the DOAS method has been improved rapidly and is mainly applied in atmospheric research. The DOAS technique is based on the absorption of ultraviolet (UV) and visible light along specific light paths by atmospheric molecules. Passive DOAS observations typically use the scattered sun light

as light source, and vertically integrated trace gas concentrations are usually retrieved. Recently, (Chen et al., 2009) introduced a detailed method for the determination of the vertically integrated tropospheric NO_2 concentration from passive DOAS observations of zenith scattered light. Active DOAS observations utilize artificial light sources, and average surface concentrations of trace gases are retrieved.

The DOAS technique has been developed to measure many atmospheric trace gases, such as O_3, NO_2, HONO, SO_2, CS_2, BrO, IO, OClO and more than 30 kinds of hydrocarbons (Febo et al., 1996; Vandaele et al., 2005; Hönninger et al., 2002; Kourtidis et al., 2000; Bruns et al., 2006, Platt and Stutz, 2008). HONO, OH, NO_3, BrO, ClO in the troposphere and OClO, BrO in the stratosphere were first measured by DOAS method, the measurement precision substantial increased during recent years (Zhou et al., 2002; Qi et al., 2002).

2 Method

2.1 Experimental

Determination of the ETMH based on the DOAS technique by combination of active DOAS and passive DOAS could be educed by analyzing of the integrated NO_2 concentrations, respectively retrieved by active DOAS and passive DOAS. The principle of active DOAS (LP-DOAS) and passive DOAS (Zenith DOAS) is shown in Fig. 1.

The light source of passive DOAS is the incoming solar irradiation. The receiving telescope is directed at the zenith sky and receives scattered sun light. Since scattered light passes through the whole atmosphere, this method provides information on the total NO_2 column density. After subtracting the stratospheric NO_2 column density and correcting for light path effects, the vertical column density (VCD, the vertically integrated concentration) in the troposphere can be determined (Chen et al., 2009). This method can be applied with good accuracy especially to observations in polluted regions. An active DOAS instrument observes light from an artificial light source over

a horizontal distance. Usually the light source is at the same location as the receiver and a retro-reflector that is placed at certain distance, folds the beam back to transmitting/receiving telescope. The light transfers a double distance between transmitting/receiving telescope and retro-reflector, and thus active DOAS offers the possibility to measure the integrated concentration of air pollutants in the lower atmosphere as is presented in Fig. 1 (Platt et al., 1994, 2008; Noxon, 1975; Zhou et al., 2005). The average trace gas concentration along the optical path can be derived by dividing the integrated concentration by the length of the path.

2.2 Calculation of the effective trace gas mixing height

The basic assumption of our new technique for the determination of the ETMH is that the NO_2 is completely mixed in mixing layer, and its profile along with altitude can be approximated by that shown in Fig. 2.

For simplicity we then can assume that the NO_2 concentration is constant within the MH and zero above. Then $N_{LP\text{-}DOAS}$ retrieved from active DOAS and VCD_{ETMH} retrieved from passive DOAS are directly connected via the ETMH, which can be obtained by the following formula:

$$ETMH = \frac{VCD_{ETMH}}{N_{lp\text{-}DOAS}}. \quad (1)$$

The following example illustrates how to calculate the ETMH with this method. Figure 3 shows a comparison between results from active DOAS and passive DOAS; active DOAS data has been converted into VCD_{EMTH} through multiplying by the ETMH. In Fig. 3a, the ETMH is assumed as 0.3 km. It is found that the result of active DOAS is close to that from the passive DOAS at 8:00 and from 16:00 to 17:00. Thus we can say that our observations are in agreement with an ETMH of 0.3 km at these times. Figure 3b, c show similar comparisons for assumed ETMH of 0.6 km and 0.8 km, respectively. Good agreement with the VCD_{EMTH} is found for other periods of the day.

AMTD
2, 1663–1692, 2009

The above analysis confirms our basic assumptions, and yields results for the diurnal variation of the ETMH which are in general agreement with expectations.

It should be noted that instead of assuming a vertically constant trace gas concentration, a constant mixing ratio would be more realistic. However, for simplicity we chose a constant concentration in this first study. Since the boundary layer is usually confined to the lowest 1–2 km, the resulting errors are small, and probably usually smaller than other uncertainties. The method can in principle easily be extended using the assumption of vertically constant mixing ratio.

3 Results

To reduce a possible cloud influence on the results of passive DOAS, only observations for mainly cloud free conditions were selected. The selection was performed according to the simultaneously observed O_4 absorptions (Chen et al., 2009).

Experiment is paused in July and August because of school vacation. As a result, there are valid data for 93 days during the whole year. Table 1 shows the distribution of measurement days in different months. According to weather condition and season, the experiment is operated from 5:00 to 18:00 every day. In total 1017 data points of hourly averages are obtained during that period. From the hourly averaged data monthly averages (Figs. 4, 5) are calculated. Except the values in January, both the seasonal and diurnal variation of the ETMH shows the expected dependence: low values occur in winter and in the morning as well as high values in summer and at noon and afternoon.

The high values in January are probably caused by the long lifetime of NO_x in the troposphere during winter. Under such conditions, local measurements can be strongly influenced by emissions from distant sources. Since the method relies on the assumption of rapid mixing of local emissions, measurement results retrieved under such conditions have to be treated with care (for more details see Sect. 4.3).

Due to limited space, it is impossible to illustrate every day's data. We will systematically discuss them in the next section.

4 Discussion

Mixing layer height is governed by many factors and follows a systematic seasonal variation. Meteorological parameters strongly affect the MH, especially surface temperature, wind speed, and wind direction. In this section we investigate the correlation between meteorological parameters and the ETMH.

4.1 Correlation between the ETMH and surface temperature

The variation of surface temperature controls the occurrence of atmospheric convection, so surface temperature changes have a strong effect on the MH. This relationship is well demonstrated for the observations from 11 May 2007 (see Fig. 6). It is expected that surface temperature should have the strongest effect in summer, when the solar irradiation is strongest and days are longest in the northern hemisphere. This expectation is broadly confirmed by the results shown in Table 2. The correlation coefficients between the ETMH and surface temperatures are highest in autumn and summer and smallest in winter and spring.

The monthly variation of the correlation coefficients between the ETMH and temperature is also presented in Fig. 7. It's a box figure, each box represents each month, where lower and higher boundaries are the 25 and 75 percentiles. The median value and the mean concentrations are respectively the solid lines and hollow squares. The low and high external lines represent the 90 and 10 percentiles while the maximum and minimum values are marked with stars outside the boxes. This graph gives more details of the data.

It can be seen in Fig. 7, that the range of means is between 0.4 and 0.84, the lowest mean occurs in December, when the minimum is −0.818, much less than other data of

this month. But if we pay attention to the median, it can be found that the range is only from about 0.51 to 0.83. The lowest median appears in January, while, the highest is in September (in January and December, the median is close to the lower boundaries of the boxes). It should be mentioned that, because there are too little data in March, June and October, no median is calculated in those months.

In January and February, the correlation between the ETMH and temperature is a little bit lower than in other months. This might be related to the fact that in those months, the temperature is lower compared with other months, so other meteorological parameters, such as wind speed and wind direction may have a more dominant effect on the ETMH than in other months.

Although in general surface temperature has a large impact on the mixing layer, other factors play a leading role in some cases. Then the relationship between the ETMH and temperature is low. For instance, the value is −0.818 on 2 December 2007, which illuminates the ETMH variation is opposite to temperature, and other meteorological factors are the dominant ones.

4.2 Correlation between the ETMH and surface wind speed

Wind Speed (WS) is found to be another important factor impacting the MH. Similar to the correlation analysis between the ETMH and temperature, that of ETMH and WS is calculated and analyzed. Table 3 show the results of the correlation retrieved between both quantities. The correlation coefficients are highest for winter indicating that the wind speed plays a dominant role in seasons with little solar irradiation.

The box graph of the correlation coefficients between ETMH and WS is also shown in Fig. 8. We can see in this graph, that all the means are in the range of 0.22 and 0.54, much lower than those between ETMH and temperature. The median ranges from 0.24 to 0.72, the maximum median occurs in April. The dynamic range is larger than that between the ETMH and temperature, which indicates that in some cases, wind can dominate the ETMH, but this does not happen frequently. This also can be seen from the difference of maximum and minimum in each month.

In contrast to the correlation between the ETMH and temperature, the correlation between the ETMH and wind speed in the cold season is in general larger than in the warm season. This indicates that in winter WS has a stronger effect on the ETMH than in summer.

On the basis of the correlation analyses, different days can be classified with respect to four situations: a) both temperature and WS show good correlation with the ETMH, as for instance on 8 May, 29 November, 13 May; b) correlation of the ETMH with temperature is high, but with WS is rather low, as for instance on 14 May, 9 November, 22 November. The occurrence of cases a) and b) are quite frequent; c) correlation of the ETMH with WS is high, but with temperature is rather low, as for instance on 2 December. This case hardly appeared; d) Not only temperature but also WS is irrelevant to the ETMH, as for example on 7 and 8 December. Also the probability for case d) is very small. For these cases, other factors than temperature and WS, for example wind Direction (WD), relative humidity (RH) and pressure (p), might play a dominant role.

4.3 Influence of atmospheric lifetime on the determination of the ETMH

The proposed method to determine the ETMH depends on two major assumptions. First, on the occurrence of an effective mixing of pollutants throughout the whole mixing layer. Second, on the fact that the local conditions are not significantly affected by pollutants from distant sources. The second point can become important especially during winter time, because usually a) higher wind speeds appear and b) the NO_x lifetime becomes substantially longer. Under such conditions distant sources can have a strong influence on our new method. To investigate these effects in more detail, we selected the period from 6 to 10 January. Figure 9 describes the variation of the ETMH, temperature, WS, RH and pressure from 6 to 10 January.

During the first part of the selected period unrealistically high ETMH were observed. For these observations, temperature was low and wind speed rather high. We also calculated back trajectories [http://www.ready.noaa.gov/hysplitarc-bin/traj1file.pl?

metdata=GDAS1] (see Fig. 10) and found that for 6 to 8 January the air masses came indeed from polluted sources.

In contrast, on 9 and 10 January, the air masses traversed the ocean before they arrived over the measurement site (see Fig. 10). Thus they carried less pollution compared to the period from 6 to 8 January. Together with the data on WS and WD we thus can explain the reason why the ETMH of the first days is larger than on the following days. The observations in January 2008 indicate a general limitation of our method, which is most pronounced in winter. Under such conditions, the passive DOAS might observe NO_2 at higher altitude, which is transported from distant sources but which can not be observed by the active DOAS. This effect will lead to an overestimation of the ETMH according to Eq. (1).

4.4 Comparison with other results

Yang et al. studied resent 15 years MH variation at 2:00, 8:00, 14:00 and 20:00 from 1990 to 2004 in Shanghai (Yang et al., 2006). In their study, daily MH were calculated based on atmospheric stability and wind speed on the surface (10 m above ground) according to the national standard (GB/T 13201∼91) of China. Unfortunately, there is no temporal overlap between their results and our observations. However, since Yang's results are 15 years averages, they might well be representative for the seasonal variation of the ETMH in Shanghai. In Table 4, we compare the ETMH at t 8:00 and 14:00 with their results (see also Fig. 4).

The ETMH derived from the DOAS observations is nearly 22% lower than the mean MH at 8:00, but it is about 14% larger at 14:00. However, it should be noted that in Yang's results also substantial differences are found for different years: the minimum of the MH appeared in 1995 (0.57 km at 8:00 and 0.82 km at 14:00), while the maximum appeared in 2004 (0.68 km and 0.91 km at 8:00 and 14:00, respectively).

Taking into account that the ETMH and MH are derived by two completely different methods, the differences between both data sets are rather small.

Figure 11 shows the annually averaged daily variation of the ETMH from 7:00 to

16:00 in 2007 (A). The maximum of the ETMH occurs is at 14:00. This is similar to the results from Yang et al. (B).

5 Errors of the method

Errors of the ETMH derived from the combination of active DOAS and passive DOAS origin from uncertainties of the assumed NO_2 vertical distribution profile and measurement errors of the two instrument themselves.

As shown in Fig. 1, our method is based on the assumption of a specified vertical profile; in our case a constant NO_2 concentration was assumed. Of course, the real profile will in general differ from this assumed profile. An additional, but associated error results from the fact that the passive DOAS detects NO_2 not only in the mixing layer but also in the free troposphere. If considerable NO_2 exists in free troposphere, it will be erroneously regarded as being in the mixing layer. Consequently, this effect leads to an overestimation of the retrieved ETMH. Suppose that the NO_2 concentration in the free troposphere is 2 of that in the mixing layer and that the free troposphere is five times as high as the mixing layer. The resulting error of the retrieved ETMH according to Eq. (3) would be 10%. As mentioned above, if temperature in winter is low and wind comes from inland high-polluted areas, it will bring NO_2 to Shanghai, part of it might be present at high altitudes in the free troposphere. This can lead to a strong overestimation of the true ETMH (see Sect. 4.3).

If the concentration of NO_2 is small, measurement errors of the instruments themselves can become the dominating error source. The uncertainty of the passive DOAS instrument is about >50% for NO_2 VCDs$<0.5\times10^{16}$ molec/cm^2. That means that for VCD_{ETMH} in that range or below, the uncertainties of the method becomes larger than 50%. Note, however, that in Shanghai, typical VCD_{ETMH} are by far larger and the respective errors are smaller (Chen et al., 2009).

Similarly, also for low surface concentrations derived from the active DOAS, the uncertainties of the ETMH increase, since this quantity appears in the denominator of

AMTD
2, 1663–1692, 2009

Eq. (1). This might become especially important if a systematic bias exists for the data from the active DOAS. For low values of the analysed surface concentrations, even small systematic biases can lead to strong systematic deviations of the derived ETMH. This might be one potential reason for the rather high values of the ETMH in May (see Fig. 5). In those months many observations of the active DOAS yielded rather small surface concentrations of NO_2.

In addition to vertical gradients of the NO_2 concentration within the mixing layer, also horizontal gradients affect the retrieval. If, for example, an air mass with higher NO_2 concentration emerges at low altitude over the measurement site, it will increase the results of the active DOAS leading to an underestimation of the MH. However, since in this study hourly averages are used, this effect should be rather small.

6 Conclusions

We introduced a new method for the determination of the mixing layer height by combination of active DOAS and passive DOAS observations of NO_2. In contrast to conventional definitions of the mixing layer height, our method is sensitive to the vertical distribution of trace gases; thus we refer to the retrieved layer height as an "effective trace gas mixing height" (ETMH). Depending on the atmospheric lifetime and vertical exchange, the ETMH could differ systematically from the meteorological mixing layer height. However, for several applications, the ETMH might be a well suited quantity, especially for studies with focus on the dispersion and transport of pollutants.

We analysed trace gas observations in Shanghai over one year (1017 hourly means in 93 days in 2007), and found the ETMH to range between 0.1 km and 2.8 km (average is 0.78 km); more than 90% of the measurements yield an ETMH between 0.2 km and 2.0 km. The seasonal and diurnal variation of the ETMH shows good agreement with mixing layer heights derived from meteorological observations (Yang et al., 2006).

Finally, we investigated the relationship of the derived ETMH to temperature and wind speed and found correlation coefficients of 0.65 and 0.37, respectively. Also the

wind direction has an impact on the measurement to some extent. Especially in cases when the air flow comes from highly polluted areas and the atmospheric lifetime of NO_2 is long (e.g. in winter), the NO_2 concentration at high altitudes over the measurement site can be enhanced, which leads to an overestimation of the ETMH. Enhanced NO_2 concentrations in the free atmosphere and heterogeneity within the mixing layer can cause additional uncertainties.

Our method could be easily extended to other species like e.g. SO_2, HCHO or Glyoxal. Simultaneous studies of these molecules could yield valuable information on their respective atmospheric lifetimes.

Acknowledgements. We thank the National High-tech R&D Program of China for supporting this research. We also acknowledge Chen Dan's former research work for this study. Fund Program: supported by "863 project", No: 2006AA06Z417

References

Berman, S., Yeong, J. K., Zhang, J., and Rao, T.: Uncertainties in estimating the mixing depth – comparing three mixing-depth models with profiler measurements, Atmos. Environ., 31, 3023–3039, 1997.

Bruns, M., Buehler, S. A., Burrows, J. P., Richter, A., Rozanov, A., Wang, P., Heue, K. P., Platt, U., Pundt, I., and Wagner, T.: NO_2 Profile retrieval using airborne multi axis UV-visible skylight absorption measurements over central Europe, Atmos. Chem. Phys., 6, 3049–3058, 2006, http://www.atmos-chem-phys.net/6/3049/2006/.

Chen, D., Zhou, B., Beirle, S., Chen, L. M., and Wagner, T.: Tropospheric NO_2 column densities deduced from zenith-sky DOAS measurements in Shanghai, China, and their application to satellite validation, Atmos. Chem. Phys., 9, 3641–3662, 2009, http://www.atmos-chem-phys.net/9/3641/2009/.

Evangelisti, F., Baroncelli, A., Bonasoni, P., Giovanelli, G., and Ravegnani, F.: Differential optical absorption spectrometer for measurement of tropospheric pollutants, Appl. Optics, 34, 2737–2744, 1995.

Febo, A., Perrino, C., and Allegrini, I.: Measurement of nitrous acid in Milan, Italy, by DOAS and diffusion ednuders [J], Atmos. Environ., 30, 3599–3609, 1996.
García, M. A., S'anchez, M. L., de Torre, B., and Pérez, I. A.: Characterisation of the mixing height temporal evolution by means of a laser dial system in an urban area – intercomparison results with a model application, Ann. Geophys., 25, 2119–2124, 2007, http://www.ann-geophys.net/25/2119/2007/.
He, Q. S., Mao, J. T., Chen, J. Y., and Hu, Y. Y.: Observational and modelling studies of urban atmospheric boundary-layer height and its evolution mechanisms, Atmos. Environ., 40, 1064–1077, 2006.
Hönninger, G. and Platt, U.: The role of BrO and its vertical distribution during surface ozone depletion at Alert, Atmos. Environ., 36, 2481–2489, 2002.
Kourtidis, K., Ziomas, I., Zerefos, C., Gousopoulos, A., Balis, D., and Tzoumaka, P.: Benzene and toluene levels measured with a commercial DOAS system in Thessaloniki, Atmos. Environ., 34, 1471–1480, 2000.
Noxon, J. F.: Nitrogen dioxide in the stratosphere and troposphere measured by ground-based absorption spectroscopy, Science, 189, 547–549, 1975.
Perner, D. and Platt, U.: Detection of nitrous acid in the atmosphere by differential optical absorption, Geophys. Res. Lett., 6, 917–920, 1979.
Platt, U.: Differential optical absorption spectroscopy (DOAS), in: Air monitoring by spectroscopic techniques, edited by: Sigrist, M. W., Chem. Anal. Ser., 127, 27–84, 1994.
Platt, U. and Stutz, J.: Differential Optical Absorption Spectroscopy – Principles and Applications, Springer-Verlag Berlin Heidelberg, 2008.
Qi, F., Liu, W. Q., Zhou, B., Li, Z. B., and Chui, Y. J.: Improving DOAS System Measurement Precision with Artificial Neutral Network Method, Acta Optica Sinica, 22, 1346–1349, 2002.
Seibert, P., Beyrich, F., Gryning, S.-E., Joffre, S., Rasmussen, A., and Tercier, P.: Review and intercomparison of operational methods for the determination of the mixing height, Atmos. Environ., 34, 1001–1027, 2000.
Solomon, S., Portmann, R. W., Sanders, R. W., Daniel, J. S., Madsen, W., Bartram, B., and Dutton, E. G.: On the role of nitrogen dioxide in the absorption of solar radiation, J. Geophys. Res., 104, 12047–12058, 1999.
Vandaele, A. C., Fayt, C., Hendrick, F., Hermans, C., Humbled, F., van Roozendael, M., Gil, M., Navarro, M., Puentedura, O., Yela, M., Braathen, G., Stebel, K., Tørnkvist, K., Johnston, P., Kreher, K., Goutail, F., Mieville, A., Pommereau, J.-P., Khaikine, S., Richter, A., Oetjen, H.,

Wittrock, F., Bugarski, S., Frie, U., Pfeilsticker, K., Sinreich, R., Wagner, T., Corlett, G., and Leigh, R.: An intercomparison campaign of ground-based UV-visible measurements of NO_2, BrO, and OClO slant columns: Methods of analysis and results for NO_2, J. Geophys. Res., 110, D08305, doi:10.1029/2004JD005423, 2005.

Yang, Y. J.,Tan, J. G., Zheng, Y. F., and Cheng, S.H.: Study on the atmospheric stabilities and the thickness of atmospheric mixed layer during recent 15 years in Shanghai, Scientia Meteorolo Gica Sinica, 26, 537–541, 2006.

Zhou B., Hao, N., and Chen, L. M.: A study on the effect of Fraunhofer structure on the measurement of atmospheric pollutants with differential optical absorption spectroscopy, Acta Phys. Sin-Ch. Ed., 9, 4445–4450, 2005.

Zhou, B., Liu, W. Q., Qi, F. Li, Z. B., and Chui, Y. J., Error analysis in Differential Optical Absorption Spectroscopy, Acta Optica Sinica, 22, 957–961, 2002.

Table 1. Number of measurement days in each month.

	Jan	Feb	Mar	Apr	May	Jun	Sep	Oct	Nov	Dec
Days	7	12	4	15	12	3	7	8	15	10

Table 2. Correlation between the ETMH and surface temperature for different seasons.

Season	Correlation coefficient
Spring	0.59
Summer	0.7
Autumn	0.81
Winter	0.68

Table 3. Correlation between ETMH and wind speed for different seasons.

Season	Correlation coefficient
Spring	0.43
Summer	0.38
Autumn	0.22
Winter	0.48

Table 4. Comparison of the ETMH with the MH observed by Yang et al.

Time	Layer height (km)					
	8:00			14:00		
	min	mean	max	min	mean	max
MH (Yang Yongjie et al.)	0.57	0.63	0.68	0.82	0.86	0.91
ETMH (DOAS)	0.49 (Sd:0.19)			1.0 (Sd:0.22)		

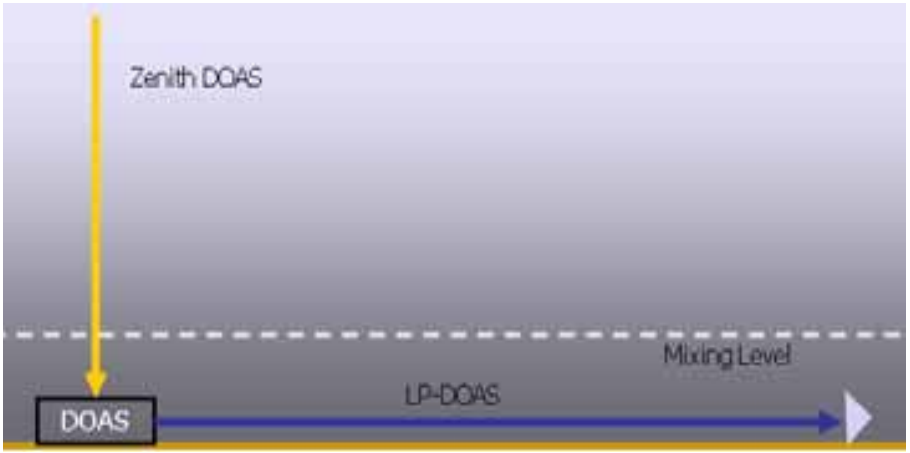

Fig. 1. Scheme of passive DOAS and active DOAS. From passive zenith sky observations, the tropospheric vertical column density is determined. From active long path observations, the average surface-near concentration is derived.

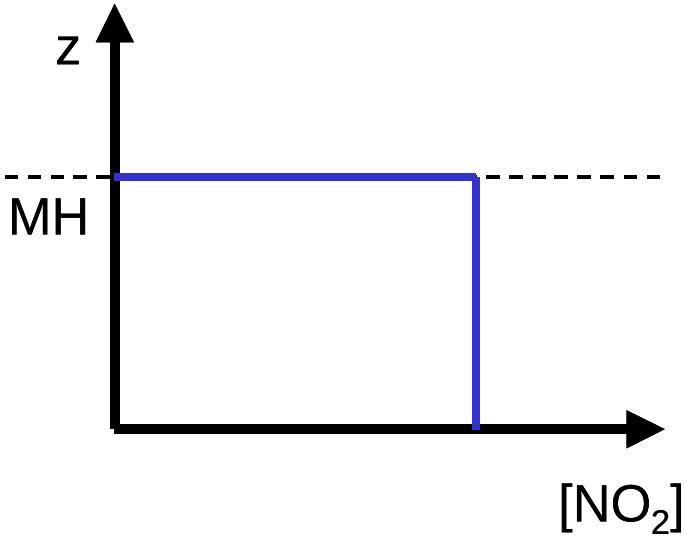

Fig. 2. Schematic tropospheric profile of NO_2 with constant concentration within the MH and zero above.

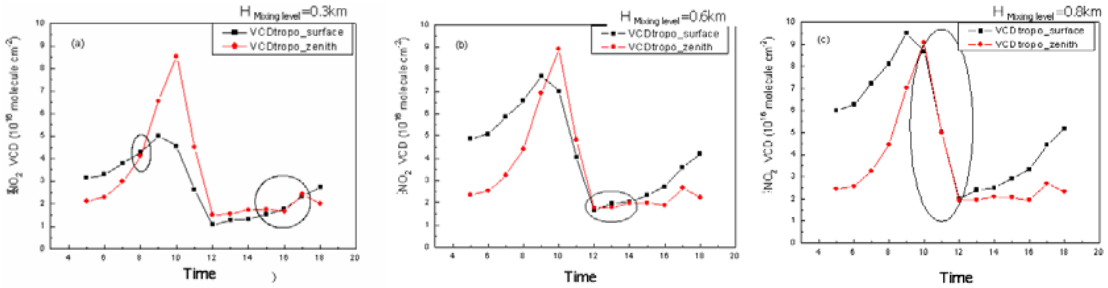

a b c

Fig. 3. Comparison of VCD_{ETML} results of active DOAS and passive DOAS for different ETMH assumptions.

AMTD
2, 1663–1692, 2009

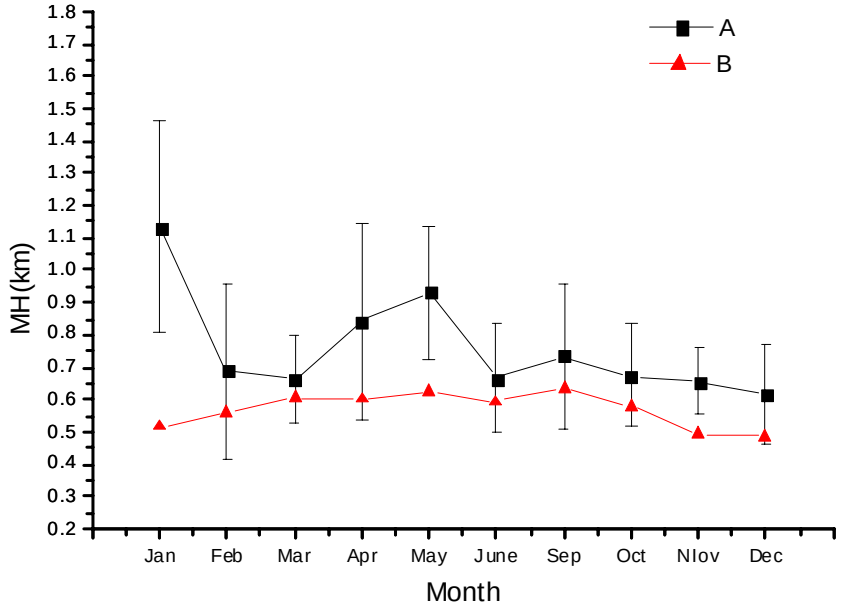

Fig. 4. **(A)** Monthly average ETMH in 2007. The error bars indicate the standard variation. Note that the high values in January overestimate the true values because of the long lifetime of tropospheric NO_x in winter (see Sect. 4.3). **(B)** Monthly average MH derived from meteorological data (Yang et al., 2006). Note that Yang's data include MH data at 2:00 and 20:00. Thus values systematically lower than ours should be expected.

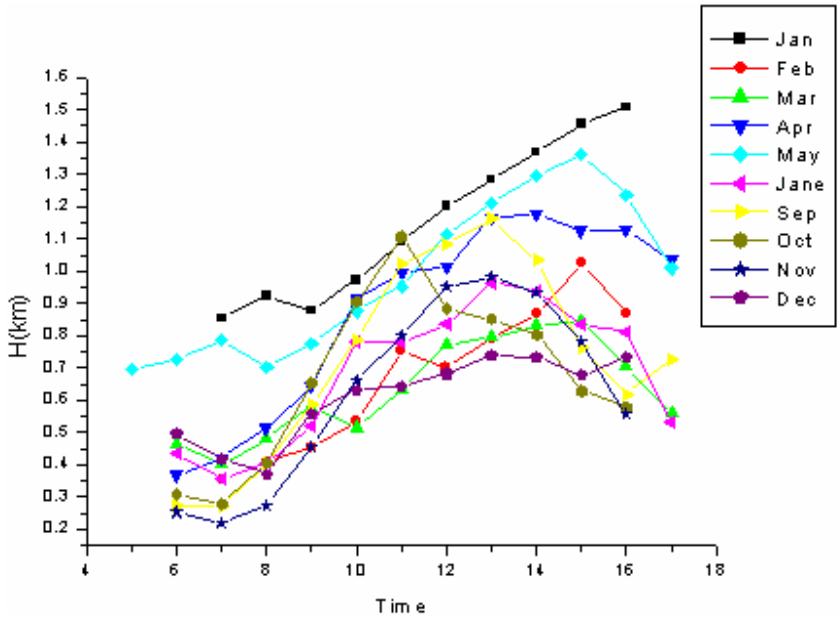

Fig. 5. Monthly averaged diurnal variation of the ETMH. Again it should be noted that the high values in January overestimate the true ETMH (see Sect. 4.3).

AMTD
2, 1663–1692, 2009

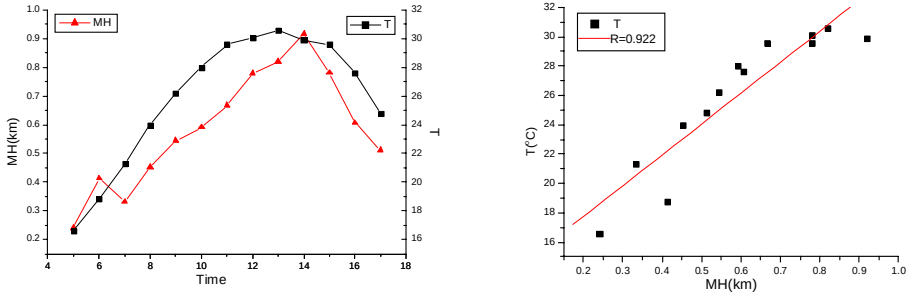

Fig. 6. Correlation between the ETMH and surface temperature.

AMTD
2, 1663–1692, 2009

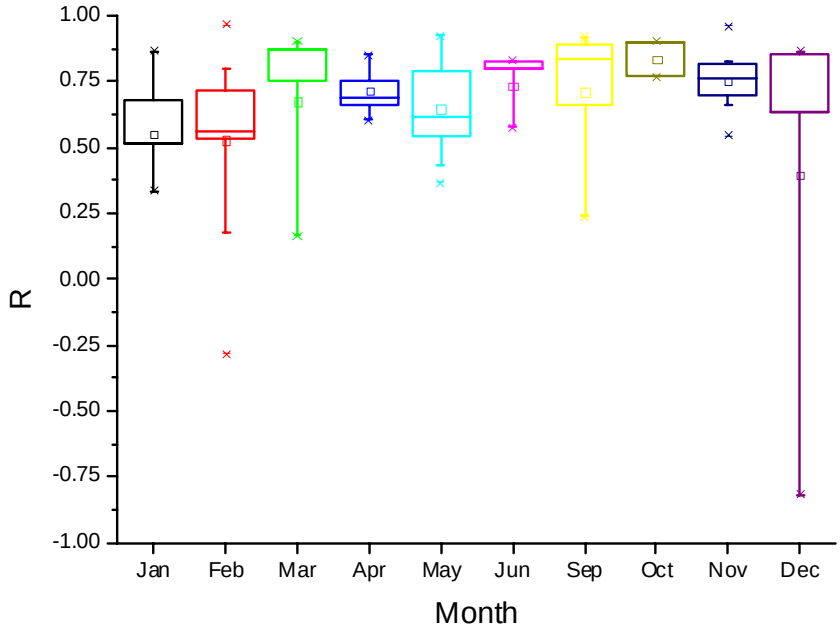

Fig. 7. Monthly variations of the correlation between the ETMH and surface temperature.

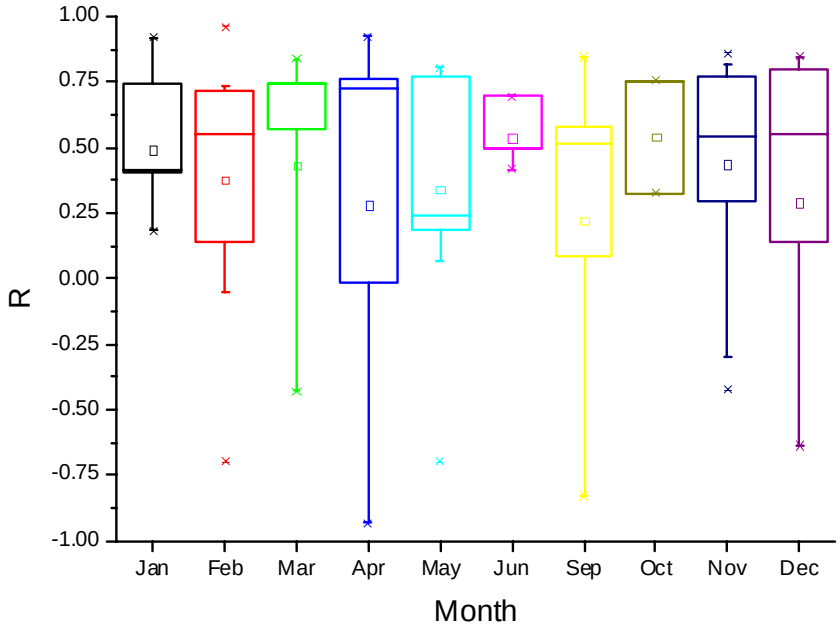

Fig. 8. Monthly variations of the correlation between the ETMH and wind speed.

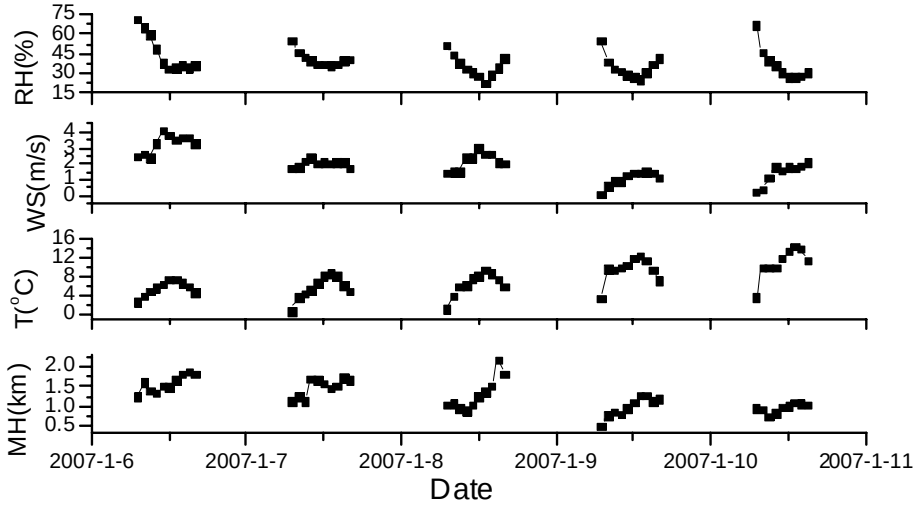

Fig. 9. Variation of the ETMH, temperature, WS, RH and pressure from sixth to tenth of January. The ETMH on 6, 7, 8 January is obviously higher than on 9 and 10 January, and even the lowest values exceed 0.88 km. This phenomenon conflicts with the expectation that both the MH and its variation is low in winter.

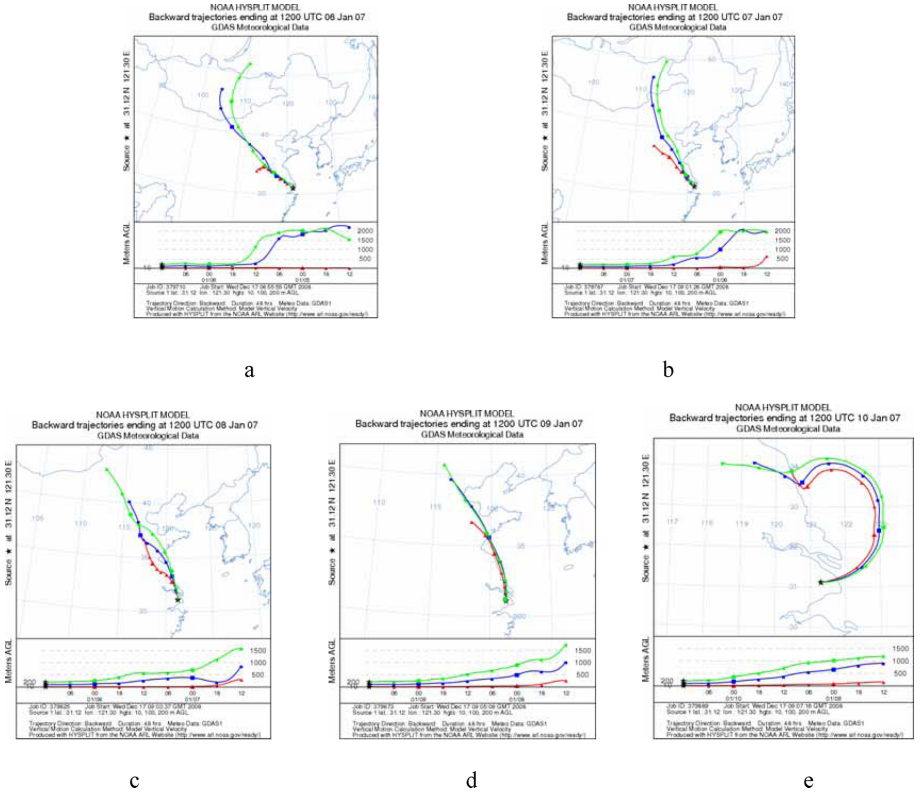

Fig. 10. Back trajectories (48 h) arriving in Shanghai from sixth to tenth **(a–e)**, January.

AMTD
2, 1663–1692, 2009

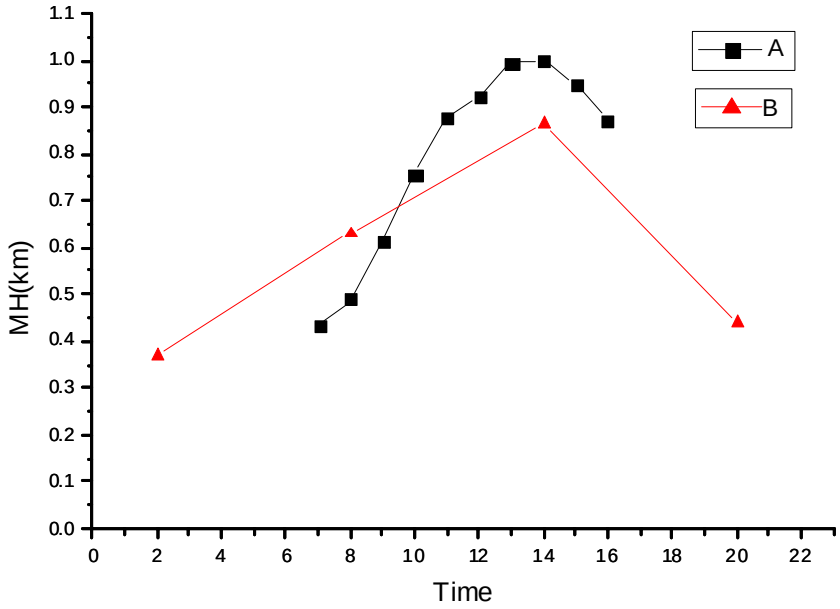

Fig. 11. Annually averaged daily variation of the ETMH in 2007 **(A)** and 15 years MH variation at 2:00, 8:00, 14:00 and 20:00 from 1990 to 2004 in Shanghai **(B)**.